A GRAPHICAL METHOD FOR PREPARING 1000-MILLIBAR PROGNOSTIC CHARTS

By Richard J. Reed

University of Washington[1]

(Manuscript received 18 June 1956)

ABSTRACT

A method is presented for preparing 1000-millibar (surface) prognostic charts. The method makes use of the graphical technique developed by Fjörtoft and is based on a baroclinic model which resembles closely that employed by Estoque in the prediction of cyclone development.

Three cases tested to date have yielded correlations of 0.93, 0.89 and 0.88 between predicted and observed 1000-mb height changes.

1. Introduction

It is now well established that numerical forecasts based on the vorticity equation compare favorably in accuracy with subjective forecasts prepared by an experienced forecaster. Currently there are two methods available for performing the numerical forecasts: (1) the arithmetical method which requires the use of a high-speed computer, and (2) the graphical method developed by Fjörtoft (1952). The graphical method has been applied with considerable success in the determination of 500-mb height changes under the barotropic assumption, and Estoque (1956) has recently extended the method to a simple baroclinic model which predicts cyclone development.[2]

To handle more complex and realistic models, high-speed computers are a necessity; therefore, in the long run, the arithmetical method should prove to be the primary method of numerical prediction. However, at present the Fjörtoft method is of practical importance to the forecaster, as evidenced by the use being made of it in various meteorological organizations. Moreover, it is a valuable aid to the instructor of meteorology in his efforts to give the student forecaster an understanding and appreciation of the newer dynamic methods of prediction. For this latter reason, if for none other, it is likely that the graphical method is destined to play an enduring role in the science of weather forecasting.

The purpose of the present article is to extend the Fjörtoft method to the problem of preparing 1000-mb (surface) prognostic charts. Estoque (1956) has already done this on the basis of what are stated to be "some rather bold assumptions". Most of these assumptions are common to other baroclinic models. The motion is assumed to be quasi-geostrophic, hydrostatic and adiabatic. A functional relationship is assumed for the vertical velocity profile, the relative vorticity is neglected relative to the Coriolis parameter in the divergence term of the vorticity equation, and the tilting term in this equation is neglected. Furthermore, the wind hodograph is assumed to be straight.

Peculiar to the Estoque model, however, is the assumption that the advection of surface vorticity by the surface wind, and also by the wind at the level of non-divergence, is small and may be neglected. This condition is tantamount to assuming that the advection of surface vorticity by the thermal wind is zero, an assumption that is particularly bad for well-developed storm systems. In the familiar Sutcliffe (1947) development equation, this advection is one of two effects which are primarily responsible for development in the field of motion.

The method presented here contains essentially the same assumptions as Estoque's, except for the rather drastic one mentioned in the preceding paragraph. This is avoided without introducing additional restrictions and without increasing significantly the number of steps in the procedure. Because the present method is free of the assumption regarding the advection of surface vorticity, it is felt that it is more suitable for teaching purposes than the Estoque method. Whether or not it will prove of greater value in operational forecasting can only be decided on the basis of extensive testing. As yet, no comparisons of the two methods have been made.

2. Theoretical development

Neglecting the tilting terms, we may write the vorticity equation in isobaric coordinates as

$$\frac{\partial}{\partial t}(\zeta + f) = - \boldsymbol{V}\cdot\boldsymbol{\nabla}(\zeta + f) - \omega\frac{\partial}{\partial p}(\zeta + f) - (\zeta + f)\boldsymbol{\nabla}\cdot\boldsymbol{V}, \quad (1)$$

where ζ is the relative vorticity, f the Coriolis parameter, $\boldsymbol{V}$ the horizontal wind velocity, and $\omega = dp/dt$

[1] Contribution No. 24, Department of Meteorology and Climatology.

[2] *Editor's note.* See also Dr. Estoque's article elsewhere in this issue of the JOURNAL.

(essentially the vertical velocity). Substitution of the continuity equation,

$$\nabla \cdot V = -\partial\omega/\partial p, \tag{2}$$

in (1) gives

$$\frac{\partial}{\partial t}(\zeta + f) = -V\cdot\nabla(\zeta + f) - \omega\frac{\partial}{\partial p}(\zeta + f) + (\zeta + f)\frac{\partial \omega}{\partial p}. \tag{3}$$

If (3) is specialized for the 1000-mb level, it assumes the form

$$\frac{\partial}{\partial t}(\zeta_0 + f) = -V_0\cdot\nabla(\zeta_0 + f) + (\zeta_0 + f)\left(\frac{\partial \omega}{\partial p}\right)_0, \tag{4}$$

where the subscript zero refers to the 1000-mb surface. The third term in (3) disappears, because of the boundary condition $\omega_0 = 0$.

Introducing next the geostrophic condition and converting to finite difference notation, we obtain the following expression for the vorticity:

$$\zeta_g = \frac{g}{f}\nabla^2 z = \frac{4gm^2}{fd^2}(\bar{z} - z). \tag{5}$$

In (5), g is the acceleration of gravity, d the grid distance, m the magnification or scale factor for the particular map projection, z the geopotential height, and $\bar{z}$ is the average geopotential height at the corners of a square with diagonals of length $2d$ centered about the point of measurement.

Upon substitution of the above condition, (4) becomes

$$\frac{\partial}{\partial t}(\bar{z}_0 - z_0) = -V_{g0}\cdot\nabla(\bar{z}_0 - z_0) - V_{g0}\frac{fd^2}{4gm^2}\cdot\nabla f - \frac{f^2d^2\omega_5}{4gm^2(p_0 - p_5)}, \tag{6}$$

or

$$\frac{\partial}{\partial t}[\bar{z}_0 - z_0 + J(\varphi)] = -V_{g0}\cdot\nabla[\bar{z}_0 - z_0 + J(\varphi)] - \frac{f^2d^2\omega_5}{4gm^2(p_0 - p_5)}, \tag{7}$$

where, following Fjörtoft (1952), we have introduced

$$J(\varphi) = \frac{\Omega^2d^2}{g}\int_0^{\varphi}\frac{\sin\varphi\cos\varphi\, d\varphi}{m^2}. \tag{8}$$

In (6) and (7), $(\partial\omega/\partial p)_0$ has been replaced by the finite difference quotient

$$\frac{\omega_5 - \omega_0}{p_5 - p_0} = -\frac{\omega_5}{p_0 - p_5}, \tag{9}$$

and ζ_0 has been neglected relative to the Coriolis parameter. The subscript "five" signifies the 500-mb level. The symbol Ω in (8) denotes the angular velocity of the earth. Since the present method later makes use of the barotropic forecast, the upper level in finite-difference formulae should be the level of non-divergence. Recent measurements by Landers (1955) make it questionable whether such a level actually exists and suggest that the level of least divergence is closer to the 700-mb level. The procedure here has been to use 500-mb data but to reduce advections in accordance with the empirical factor recommended by the Air Weather Service (1955).

It should also be pointed out that substitution of the finite-difference quotient in (9) for the vertical derivative of ω at 1000 mb is equivalent to assuming that ω varies linearly with pressure between the 1000- and 500-mb levels. The 500-mb surface is assumed to be a level of non-divergence, so that above this level ω must decrease in magnitude. However, it is not necessary to specify the form of this decrease. The linear assumption below 500 mb may be contrasted with Estoque's (1956) assumption of a sinusoidal variation and Sawyer and Bushby's (1953) choice of a parabolic law. The linear assumption was introduced initially for simplicity and has been retained because of the success of the initial forecasts. With more extensive testing, it is possible that one of the other relationships will prove superior.

Next, following Estoque, we write the adiabatic equation in the form

$$\frac{\partial z'}{\partial t} = -V_{g0}\cdot\nabla z' + \sigma(p_0 - p_5)\frac{\omega_5}{2}, \tag{10}$$

where $\sigma = \theta^{-1}(\partial z/\partial p)(\partial\theta/\partial p)$, and z' is the thickness between 500 and 1000 mb. The use of the 1000-mb wind in (10) in place of a suitable mean wind for the layer follows from the assumptions that the hodograph is straight and that the thermal wind relationship holds. Thus,

$$(V_{g0} + V_g'/2)\cdot\nabla z' = V_{g0}\cdot\nabla z',$$

where V_g' is the thermal wind between 1000 and 500 mb.

To obtain the prediction equation, (10) is multiplied by

$$K = \frac{1}{2}\frac{f^2d^2}{gm^2\sigma(p_0 - p_5)^2},$$

and added to (7), thus yielding

$$\frac{\partial}{\partial t}[\bar{z}_0 - z_0 + J(\varphi) + Kz'] = -V_{g0}\cdot\nabla[\bar{z}_0 - z_0 + J(\varphi) + Kz']. \tag{11}$$

The parameter K, which is a relatively slow varying quantity, is treated as a constant in (11).

Equation (11) expresses the conservation of the quantity $[\bar{z}_0 - z_0 + J(\varphi) + Kz']$ in the 1000-mb wind field. Since in active weather situations the surface wind undergoes rapid fluctuations, it is necessary to replace the 1000-mb wind field by one which changes more slowly if (11) is to be integrated for periods of as long as 12 to 24 hr. The new advective field is obtained by resorting to an ingenious device due to Fjörtoft (1952).

Let

$$z_0 = \bar{z}_0 + J(\varphi) + Kz' - [\bar{z}_0 - z_0 + J(\varphi) + Kz']. \quad (12)$$

Then

$$V_{g0} = \bar{V}_{g0} + c_g + KV_g' - V_g^*, \quad (13)$$

where

$$V_{g0} = -(g/f)\,\nabla z_0 \times k,$$
$$\bar{V}_{g0} = -(g/f)\,\nabla \bar{z}_0 \times k,$$
$$c_g = -(g/f)\,\nabla J(\varphi) \times k,$$
$$V_g' = -(g/f)\,\nabla z' \times k,$$

and

$$V_g^* = -(g/f)\,\nabla[\bar{z}_0 - z_0 + J(\varphi) + Kz'] \times k.$$

Thus,

$$V_{g0}\cdot\nabla[\bar{z}_0 - z_0 + J(\varphi) + Kz'] = (\bar{V}_{g0} + c_g + KV_g')\cdot\nabla[\bar{z}_0 - z_0 + J(\varphi) + Kz']. \quad (14)$$

Substituting (14) in (11), we arrive at the prediction equation,

$$\frac{\partial}{\partial t}[\bar{z}_0 - z_0 + J(\varphi) + Kz'] = -(\bar{V}_{g0} + c_g + KV_g')\cdot\nabla[\bar{z}_0 - z_0 + J(\varphi) + Kz']. \quad (15)$$

It is seen that the quantity within the brackets is advected now by the resultant of three winds, all of which vary more slowly than the surface wind.

To recover the surface height-change, (15) may be written as

$$\Delta(\bar{z}_0 - z_0 + Kz') = -A_0, \quad (16)$$

where the delta refers to the local change of the quantity in parentheses during a 12- or 24-hr period, and A_0 denotes the measured advection over the time interval. Since $z' = z_5 - z_0$, (16) becomes

$$\Delta\bar{z}_0 - \Delta z_0 + K\,\Delta z_5 - K\,\Delta z_0 = -A_0, \quad (17)$$

or

$$(K+1)\,\Delta z_0 - K\,\Delta z_5 = A_0 + \Delta\bar{z}_0. \quad (18)$$

With the foregoing notation, the 500-mb change derived from the Fjörtoft method is expressed as follows:

$$K\,\Delta z_5 = KA_5 + K\,\Delta z_5. \quad (19)$$

Equations (18) and (19) are next added, to give

$$\Delta z_0 = \frac{1}{K+1}[A_0 + KA_5 + \Delta\bar{z}_0 + K\,\Delta\bar{z}_5]. \quad (20)$$

For disturbances of normal size, it can be shown by a method of successive approximation that

$$A_0 + KA_5 + \Delta\bar{z}_0 + K\,\Delta\bar{z}_5 \approx A_0 + K\,\Delta z_5 + (\overline{A_0 + K\,\Delta z_5}).$$

Substitution of this expression in (20) leads to the final height-change equation,

$$\Delta z_0 \approx \frac{1}{K+1}[A_0 + K\,\Delta z_5 + (\overline{A_0 + K\,\Delta z_5})]. \quad (21)$$

For standard atmospheric conditions, $K = 0.6$. Therefore,

$$\Delta z_0 \approx 0.6\,[A_0 + 0.6\,\Delta z_5 + (\overline{A_0 + 0.6\,\Delta z_5})]. \quad (22)$$

3. Practical application

The steps in the full solution of (21) will first be outlined. It is suggested that these steps be followed in instructional use of the method. Once the complete method has been described, suggestions will be offered for shortening the procedure to make it feasible for routine forecasting. Some familiarity with the Fjörtoft method is assumed in the following paragraphs.

Step 1.—Average the 1000-mb heights, using a 6 deg lat grid distance. Add graphically to $\bar{z}_0$ the field of $J(\varphi)$, which for a given map projection and grid size is always the same and can be entered permanently on a transparent overlay. Table 1 gives values of $J(\varphi)$ for a Lambert conformal projection with standard parallels at 30 and 60°N, and for a grid distance of 6 deg lat at 45°N.

Step 2.—Subtract graphically the 1000-mb contours from the 500-mb contours, to obtain the thickness z'. Interpolate isopleths such that Kz' is in the same units as $\bar{z}_0$ and $J(\varphi)$. [Since for standard conditions $K = 0.6$, isopleths will be interpolated at $z' = 17{,}170$ ft, 17,330 ft, 17,500 ft, *etc.*, and labelled in 100's of feet, if isopleths of $\bar{z}_0$ and $J(\varphi)$ are at 100-ft intervals.] Add graphically the field of Kz' to $z_0 + J(\varphi)$. The chart so obtained corresponds in function to the $\bar{z}_5 + J(\varphi)$ chart of the Fjörtoft method and, because it is used for predicting surface displacements, will be referred to as the steering chart.

Step 3.—Subtract graphically the z_0 map from the steering chart to obtain $\bar{z}_0 - z_0 + J(\varphi) + Kz'$. Valuable information may be gathered visually by putting

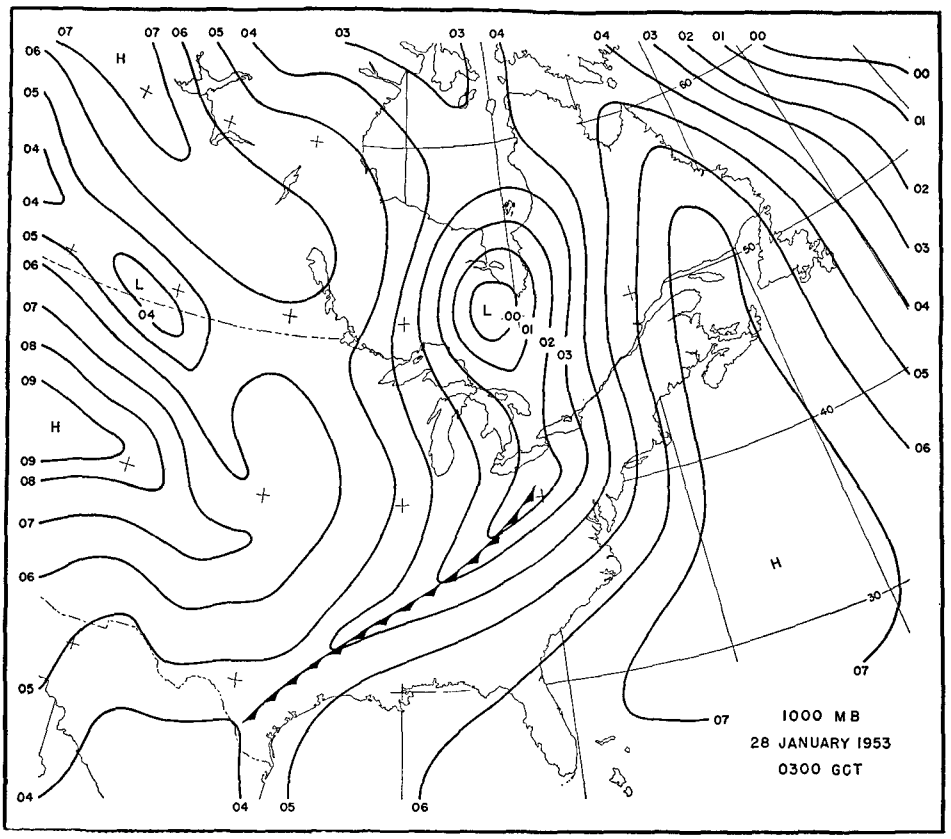

FIG. 1. 1000-mb chart for 0300 GCT 28 January 1953.

the advective lines $[\bar{z}_0 - z_0 + J(\varphi) + Kz']$ and the steering lines $[\bar{z}_0 + J(\varphi) + Kz']$ on the same overlay in different colors.

Step 4.—Advect the isopleths of $\bar{z}_0 - z_0 + J(\varphi) + Kz'$ with 80 per cent of the geostrophic wind measured from the steering chart. The 80-percent figure is recommended for the Fjörtoft method [see Air Weather Service (1955)], to compensate for the use of the 500-mb level as the level of non-divergence. The same compensation is recommended in the present method. The time interval over which the integration is performed will depend on how fast the steering flow is changing. Preliminary tests with a 12-hr interval have yielded excellent results, so that in many instances a 24-hr interval may prove permissible.

Step 5.—Subtract graphically the final $\bar{z}_0 - z_0 + J(\varphi) + Kz'$ field from the initial, to obtain A_0. Add to A_0, $K\,\Delta z_5$ as determined from the Fjörtoft method.

Step 6.—Average $A_0 + K\,\Delta z_5$ and add to $A_0 + K\,\Delta z_5$ itself. By graphical interpolation, take six-tenths of the sum. The interpolated lines give the 1000-mb height change and may be added to the initial 1000-mb chart to obtain the prognostic chart.

The suggested shortcuts for operational use of the method are as follows:

1. Neglect $J(\varphi)$ and c_φ, since in most cases they will only slightly modify the results.

TABLE 1. Latitudes of isopleths of $J(\varphi)$ at 100-ft intervals for Lambert conformal projection with standard parallels at 30 and 60°N and grid distance of 6 deg lat at 45°N.

$J(\varphi)$ (ft)	0	100	200	300
Latitude (deg)	0	33	46	60

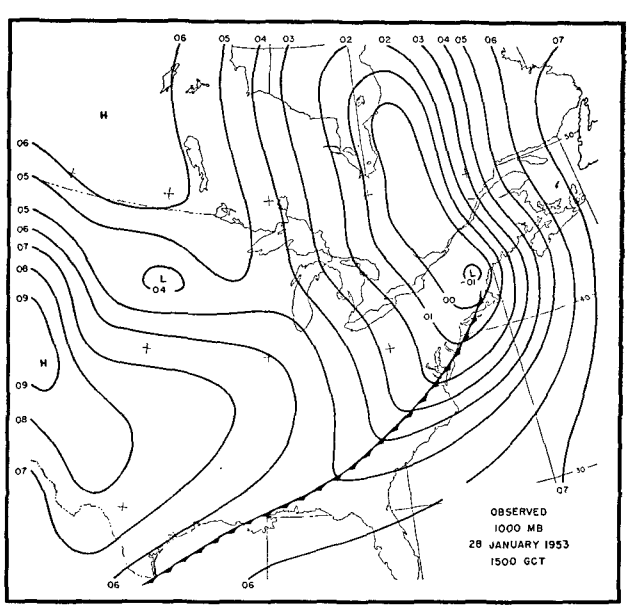

FIG. 2. Verification. 1000-mb chart for 1500 GCT 28 January 1953.

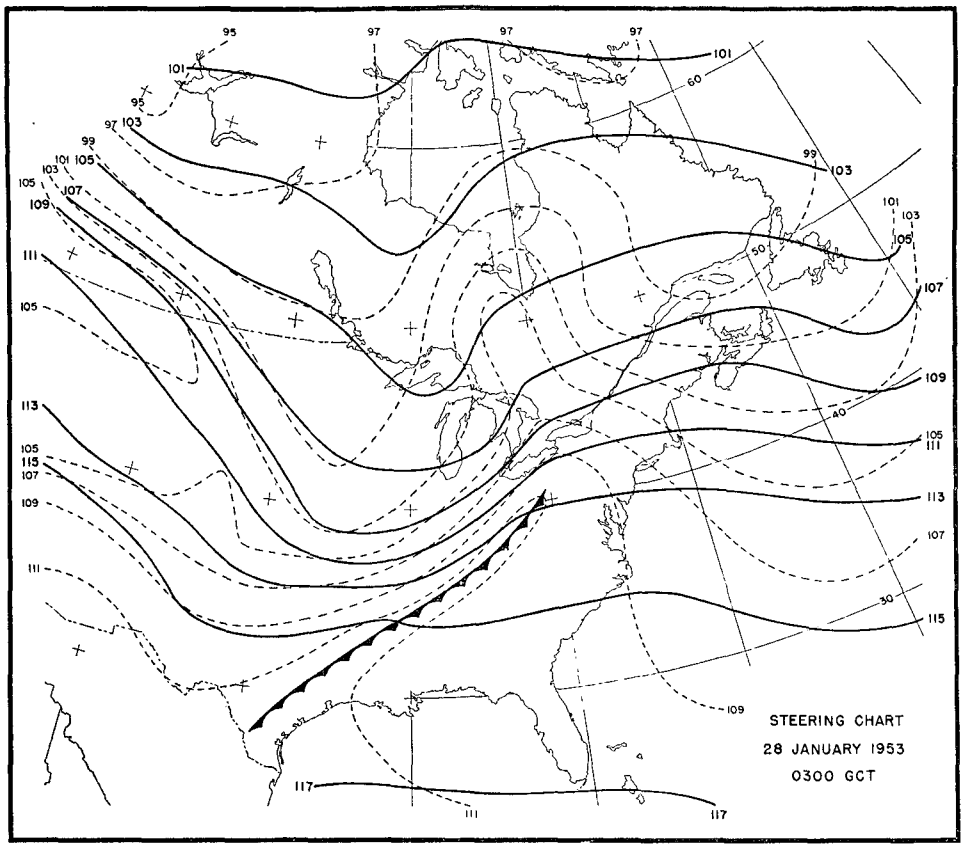

FIG. 3. Steering chart for 0300 GCT 28 January 1953. Solid lines, isopleths of $\bar{z}_0 + 0.6\,z'$. Dashed lines, isopleths of $\bar{z}_0 - z_0 + 0.6\,z'$.

2. In step 2, use $K = 0.5$ instead of 0.6. Then the graphical multiplication of K by z' is accomplished by taking every second thickness line.

3. Since K will be only five-sixths of its normal value, compensate in step 4 by advecting with the total geostrophic wind rather than with 80 per cent of the geostrophic value.

4. Eliminate the averaging in step 6 by assuming that $\overline{A_0 + K\,\Delta z_5}$ is approximately equal to $(A_0 + K\,A_5)/2$. This approximation has been suggested by the preliminary testing of the method.

Thus, in the short method, (15) simplifies to

$$\frac{\partial}{\partial t}(\bar{z}_0 - z_0 + z'/2) = -(\bar{V}_{g0} + V_g'/2)\cdot\nabla(\bar{z}_0 - z_0 + z'/2), \quad (23)$$

and (21) to

$$\Delta z_0 = A_0 + \tfrac{1}{2}A_5. \quad (24)$$

4. Results of preliminary tests

Three 12-hr forecasts have been carried out by the method so far. Table 2 gives the correlations between observed and predicted 1000-mb height changes for the three cases and the root-mean-square errors. Values were read from grid points spaced 400 km apart. For the case of 1500 GCT 14 December 1953, the original maps were analyzed for the area enclosed between latitudes 20 and 60°N and longitudes 55 and 115°W. For the other two cases, the analyses were extended slightly further to the north and west. Performance of the bar operation reduced the area of analysis by 6 deg lat on each side; and step 4 in the procedure, the advective operation, resulted in a further shrinkage of area. Thus it was possible to verify the forecasts over only a fraction of the initial area. Since the numbers entering into the correlations were read at grid points spaced 400 km apart, the variation in number of check points in table 2 from 27 to 44 corresponds roughly to a range in size of verification area of between 3 and 5×10^6 km^2. The correlations are extremely high, although it must be kept in mind that the forecasts are for a shorter time period than is ordinarily used in numerical prediction studies. The short period was chosen because it was the purpose of the preliminary testing to determine the suitability of the method as a teaching aid rather than as a forecast tool.

TABLE 2. Correlations between observed and predicted 12-hr 1000-mb height changes and root-mean-square errors.

Case	Number of points	Correlation	Root-mean-square error
0300 GCT 14 Dec 1953	42	0.89	120 (ft)
1500 GCT 14 Dec 1953	27	0.93	140
0300 GCT 28 Jan 1953	44	0.88	110

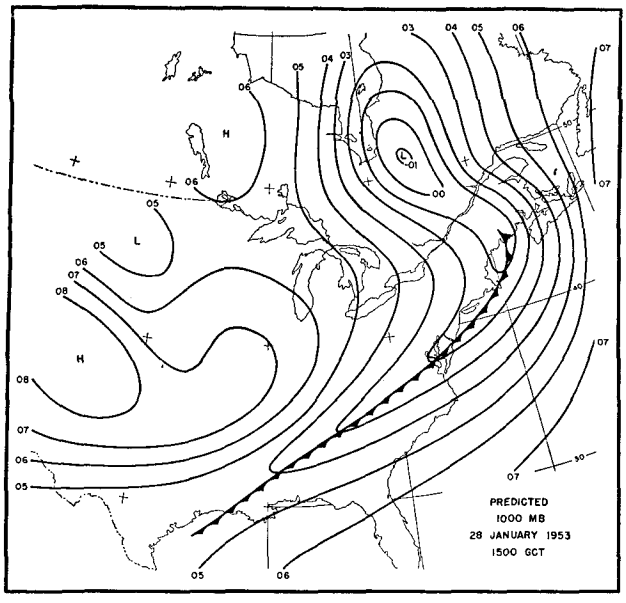

FIG. 4. 1000-mb prognostic chart for period 0300 GCT 28 January 1953 to 1500 GCT 28 January 1953.

Figs. 1 to 4 show a number of charts for the case of 28 January 1953. On the initial 1000-mb chart (fig. 1), a primary low is centered near the southern tip of Hudson Bay, a secondary low is developing near Pittsburgh, Pa., and a sharp cold front extends southwestward from this low. A minor low is present on the Montana-Saskatchewan border. The prognostic chart for 12 hr later is shown in fig. 4 and the verification in fig. 2. A few minor discrepancies between predicted and observed charts will be noted, but on the whole the agreement is good. It is interesting to note that the numerical method forecast the lower portion of the front to advance eastward at 15 kn across east Texas and Louisiana, despite the fact that the normal component of the surface geostrophic wind was close to zero. The actual frontal speed in that area was 20 kn.

The steering chart appears in fig. 3. The various lows are distinguished as ridges or domes of high value in the isopleths of $\bar{z}_0 - z_0 + 0.6\,z'$, the cold front as a long, narrow ridge. The steering flow predicts an east to east-northeast direction of movement for the eastern lows, and a southeastward motion for the low in the west. The intensity of the height rises and falls can be estimated visually by noting the size of the parallelograms formed by the intersections of the two sets of lines. Where the areas are small, the height changes are large.

The displacement of the front can be estimated quickly from the average spacing of the steering lines above and downwind from the front. The decreased spacing to the north indicates that the upper portion of the front will move faster than the lower.

From the preceding discussion, it is apparent that the steering chart may be of value to the forecaster even if used only qualitatively or semi-quantitatively. Two analysts working simultaneously can prepare this chart in less than 1 hr. With the help of an additional assistant, all steps in the short method can be accomplished in about 2 hr.

5. Concluding remarks

Encouraging results have been obtained from the three cases tested to date. However, the true test of the method must come in its application to the daily run of weather situations rather than to selected cases. For this reason, it is hoped that organizations which currently use the Fjörtoft method on a regular basis will give the present method a trial. The additional work involved should require the services of one analyst experienced in graphical techniques, and an assistant. All except the final steps in the method can be carried on simultaneously with the Fjörtoft computations.

The most obvious defect of the method which has appeared in the cases tested to date has been the tendency for ridges to thrust in behind the low centers, contrary to the observed conditions. In each case this situation has been attributable, at least in part, to the inability of the Fjörtoft method to predict deepening of the 500-mb trough. Before completely successful surface forecasts can be made, it is apparent that some way must be found to forecast development at the upper level.

Acknowledgments.—The writer wishes to thank Mr. Edwin Danielsen for his assistance in determining the recovery formula, and Miss Florence Cochrane for drafting the figures.

REFERENCES

Air Weather Service, 1955: *Fjörtoft's graphical method for preparing 24-hour 500-mb prognostic charts.* (Tech. Rep. 105–131), Washington, Military Air Transp. Serv., 11 pp.

Estoque, M. A., 1956: A prediction model for cyclone development integrated by Fjörtoft's method. *J. Meteor.*, **13**, 195–202.

Fjörtoft, R., 1952: On a numerical method of integrating the barotropic vorticity equation. *Tellus*, **4**, 179–194.

Landers, H., 1955: A three-dimensional study of the horizontal velocity divergence. *J. Meteor.*, **12**, 415–427.

Sawyer, J. S., and F. H. Bushby, 1953: A baroclinic model suitable for numerical integration. *J. Meteor.*, **10**, 54–59.

Sutcliffe, R. C., 1947: A contribution to the problem of development. *Quart. J. r. meteor. Soc.*, **73**, 370–383.